Characteristics of Nucleation and Growth Events of Ultrafine Particles Measured in Rochester, NY

CHEOL-HEON JEONG,[†] PHILIP K. HOPKE,[*,†,‡] DAVID CHALUPA,[§] AND MARK UTELL[§]

Department of Civil and Environmental Engineering and Department of Chemical Engineering and Center for Air Resources Engineering and Science, Clarkson University, Potsdam, New York 13699-5708, and University of Rochester Medical Center, 601 Elmwood Avenue, Rochester, New York 14642

Number concentrations and size distributions of particles in the size range of 0.010−0.500 μm were measured in Rochester, NY, from December 2001 to December 2002. The relationships between the number concentrations, gaseous pollutants, and meteorological parameters were examined during particle nucleation events. More than 70% of measured total number concentration was associated with ultrafine particles (UFP, 0.011−0.050 μm). Morning nucleation events typically peaking UFP number concentrations at around 08:00 were apparent in winter months with CO increases. These particles appear to be formed following direct emissions from motor vehicles during morning rush hour. There were also often observed increases in this smaller-sized range particles in the late afternoon during the afternoon rush hour, particularly in winter when the mixing heights remain lower than in summer. Strong afternoon nucleation events (>30,000 cm^{-3}) peaking at around 13:00 were more likely to occur in spiring and summer months. During the prominent nucleation events, peaks of SO_2 were strongly associated with the number concentrations of UFP, whereas there were no significant correlations between these events and $PM_{2.5}$ and CO. Increased SO_2 concentrations were observed when the wind direction was northwesterly where three SO_2 sources were located. It is hypothesized that UFP formed during the events are sulfuric acid and water from the oxidation of SO_2. There were also a more limited number of nucleation events followed by particle growth up to approximately 0.1 μm over periods of up to 18 h. The nucleation and growth events tended to be common in spring months especially in April.

Introduction

Ambient particulate matter (PM) is a complex mixture divided into coarse particles, fine or accumulation particles, and ultrafine particles (UFP, particle diameter < 0.1 μm). PM is receiving more attention in recent years as a factor in possible adverse health outcomes. Recently, numerous epidemiological and laboratory studies have shown relationships between adverse human health effects such as increased mortality, morbidity, respiratory symptoms, and PM. The observed adverse health effects were closely associated with increased mass concentration of particles smaller than 10 μm (PM_{10}) or 2.5 μm ($PM_{2.5}$) (*1*−*3*). Several inhalation and epidemiological studies suggest the adverse health effects of UFP (*4*−*12*). These studies found that UFP that penetrated pulmonary spaces can provoke inflammation and exacerbate cardiovascular symptoms or the respiratory health of asthmatic patients even if the mass concentration of the UFP was low.

Interest in size and number measurements of UFP has increased because the number size distribution of urban aerosols is dominated by the UFP, although these particles contribute very little to the total mass concentration, and particle count measurements might provide a better indication of human exposure to UFP. Recently the UFP size distributions and number concentrations in urban air have been measured at different locations (*13*−*19*). However, long-term measurements of UFP to identify the complex formation mechanisms and characterize their variability have not been widely done. The variability of the UFP number concentration in remote sites has been intensively studied at a high-alpine site in Switzerland (*20*) and at several rural sites in Finland (*21*−*23*). Limited long-term data in urban atmospheres are currently available from the United States (*24*, *25*), cities of Europe (*23*, *26*−*28*), and Brisbane, Australia (*29*, *30*), while many spatial and temporal studies measuring $PM_{2.5}$ and PM_{10} have been conducted. The study of the spatial and temporal variations of UFP is needed to examine the relationship between the UFP number concentration and human health effects.

In this paper, the number concentrations of UFP in Rochester, NY, were measured to obtain a database to define the temporal and seasonal variations over an extended time interval. These data can be used to examine the variations in particle number size distribution, the occurrence of nucleation and growth events of UFP, and the relationship of these events with other measured pollutants. The nucleation events are characterized, and the effects of gaseous pollutants and meteorological parameters on the nucleation events are examined. In addition, the contribution of local sources to the UFP concentrations will be discussed.

Experimental Methods

Measurements of particles in the size range of 0.010−0.500 μm were conducted from December 2001 to December 2002 at the NYS DEC monitoring site surrounded by an inner loop road within 0.5 mi of downtown Rochester, NY (latitude 43°09′40″ N, longitude 77°36′12″ W). It is located on approximately 50 m from major roads. Sampling was performed on the roof of the central fire station, about 10 m in height. A large coal-fired power plant is located around 6 km northwest of the sampling site. $PM_{2.5}$, SO_2, and CO concentrations; wind speed; and wind direction were measured at this location while ozone (O_3), ambient temperature, and relative humidity (RH) were obtained from another NYS DEC Rochester site (latitude 43°09′56″ N, longitude 77°33′15″ W). The locations of the monitoring sites are shown in Figure 1.

The number size distribution concentrations of fine and ultrafine particles were measured using a scanning mobility particle sizer (SMPS), consisting of a differential mobility

* Corresponding author e-mail: hopkepk@clarkson.edu; phone: (315)268-3861; fax: (315)268-6654.

[†] Department of Civil and Environmental Engineering, Clarkson University.

[‡] Department of Chemical Engineering and Center for Air Resources Engineering and Science, Clarkson University.

[§] University of Rochester Medical Center.

10.1021/es034811p CCC: $27.50
Published on Web 02/21/2004

FIGURE 1. Locations of sampling sites in Rochester, NY.

analyzer (DMA, model 3071, TSI Inc.) and a condensation particle counter (CPC, model 3010, TSI Inc.). The mobility diameter range of 0.010−0.500 μm was scanned by the SMPS over 5-min intervals. The particle size distribution data were recorded on a personal computer (PC) located at the monitoring site and were downloaded via modem to Clarkson University. Routine maintenance such as calibrating the flow rates is being performed once a week. At the beginning of the measurement period, frequent failures to download the data resulted in only 56% capture of the data for December 2001. Due to the maintenance of the SMPS system and PC failure, the coverage of the data in May and October 2002 was 76% and 74%, respectively, while the average coverage of the data from January 2002 to December 2002 was 91%. To minimize instrument uncertainties, the lowest range (0.010−0.011 μm) and the highest range (0.470−0.500 μm) of size distribution were excluded. The number concentrations were classified and calculated as a function of the three size ranges, 0.011−0.050 μm (N_{11-50}), 0.050−0.100 μm (N_{50-100}), and 0.100−0.470 μm ($N_{100-470}$), to characterize the variation of size ranges in a manner similar to that done by Wichmann et al. (*10*).

Continuous mass concentrations of fine particles with an aerodynamic diameter less than 2.5 μm ($PM_{2.5}$) were measured using a 50 °C tapered element oscillating microbalance (TEOM, R&P 1400a) operated by NYS DEC as well as hourly measurements of gaseous pollutants (CO, SO_2, and O_3) and meteorological parameters (wind speed, wind direction, temperature, and relative humidity). Spearman rank correlations were used to examine the relationships between pairs of measured variables.

Results and Discussion

Particle Number Size Distributions. Annual average number and volume concentrations and statistical parameters of the three size ranges in Rochester are shown in Table 1. The number concentrations of UFP in the size range of 0.011−0.050 μm (N_{11-50}) showed significant variability with a high standard deviation and accounted for approximately 71% of the total number concentration of 0.011−0.470 μm particles (N_{11-470}). The average number concentration in the 0.011−0.1 μm diameter ranges (N_{11-100}) contributed around 90% of the total number concentration. The value is comparable to those reported in European cities, where the contributions of UFP (0.010−0.100 μm) to total particle number concentration (0.010−0.500 μm) ranged from 88 to 94% (*26*, *27*). As expected, the volume concentrations were dominated by particles larger than 0.1 μm with an 87% contribution of the total volume concentration, whereas only 3% of the total volume was UFP smaller than 0.050 μm.

TABLE 1. Statistical Characteristics of Hourly Averaged Number Concentrations (cm^{-3}) and Volume Concentrations ($\mu m^3\ cm^{-3}$) of Particles in the Three Size Ranges during the Measurement Period December 2001−December 2002, in Rochester, NY

diameter (μm)[a]	0.011−0.050	0.050−0.100	0.100−0.470	0.011−0.470
		Number		
mean	5.80E+03	1.51E+03	8.80E+02	8.16E+03
median	4.54E+03	1.30E+03	7.50E+02	6.80E+03
SD	4.71E+03	1.03E+03	5.80E+02	5.49E+03
min	2.80E+02	7.00E+01	4.00E+01	5.40E+02
max	5.71E+04	1.15E+04	4.96E+03	6.14E+04
		Volume		
mean	8.70E−02	3.14E−01	2.74E+00	3.14E+00
median	7.10E−02	2.71E−01	2.18E+00	2.60E+00
SD	6.50E−02	2.18E−01	2.04E+00	2.16E+00
min	4.00E−03	1.40E−02	1.42E-01	1.80E−01
max	6.88E−01	2.28E+00	1.94E+01	1.95E+01

[a] SD, standard deviation; min, minimum; max, maximum.

The correlations between the hourly average ultrafine number concentrations in the two size ranges, 0.011−0.050 μm (N_{11-50}) and 0.100−0.470 μm ($N_{100-470}$), and $PM_{2.5}$ mass concentrations are shown in Figure 2. For comparison with the hourly $PM_{2.5}$ concentrations, the number concentration data measured for each 5-min interval were converted into the hourly averages. The correlation was calculated using the Spearman rank order correlation coefficient (r_s). As shown in Figure 2a, there was no correlation between the ultrafine particle number concentrations and $PM_{2.5}$ mass concentrations ($r_s = -0.03$), while between N_{50-100} and $PM_{2.5}$ there was

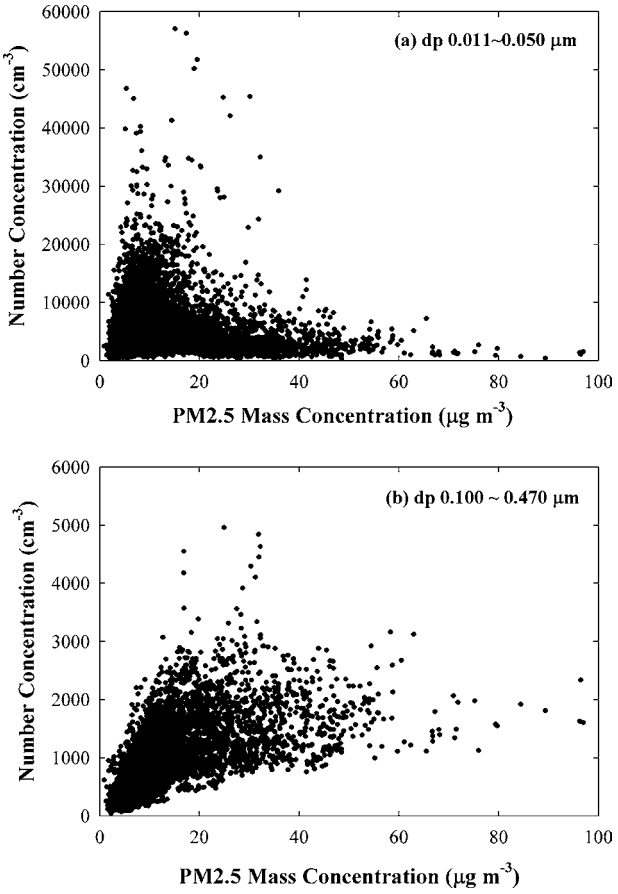

FIGURE 2. Correlation between number concentrations of particles in the size range of (a) 0.011−0.050 μm and (b) 0.100−0.470 μm and $PM_{2.5}$ mass concentrations during the measurement period of December 2001−December 2002.

a modest correlation ($r_s = 0.44$). The number concentrations of fine particles in the size range of 0.100−0.470 μm were correlated with the $PM_{2.5}$ with a correlation coefficient of 0.76 (Figure 2b). The results suggest that the collocated number measurements of UFP would be needed if their influence on human health is to be assessed.

Mass concentration of UFP could be estimated by assuming that average density was a constant 1500 kg m^{-3} and that all particles are spherical (*26*). The estimated mass concentrations of particles in the size range 0.011−0.470 μm were closely correlated with mass concentrations of $PM_{2.5}$ ($r_s = 0.82$) obtained using 50 °C TEOM, and the contribution of

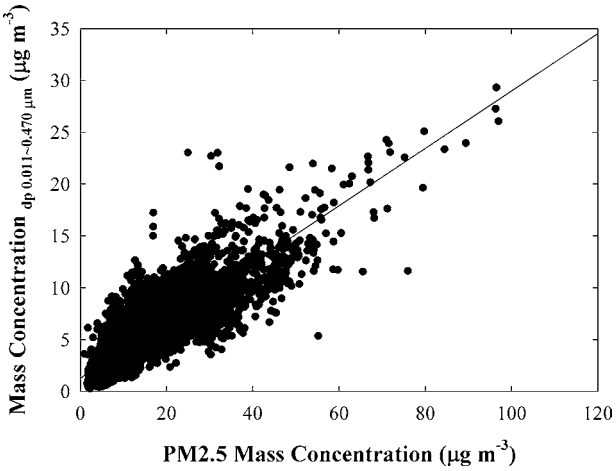

FIGURE 3. Comparison of mass concentrations of particles in the size range of 0.011− 0.470 μm estimated by using a density of 1500 kg m^{-3} and $PM_{2.5}$ mass concentrations determined with a 50 °C TEOM system.

the size range particles to the $PM_{2.5}$ mass was approximately 27% as shown in Figure 3. It should be noted, however, that there are disadvantages of the 50 °C TEOM. Several studies have reported that the 50 °C TEOM is expected to underestimate the $PM_{2.5}$ mass due to loss of semivolatile components such as ammonium nitrate and organic matter (*31*, *32*). Moreover, the amount of the evaporative losses may vary since the variation of semivolatile components may vary seasonally and spatially (*33*, *34*).

Variations of Number Concentrations. The monthly average number concentration and standard variations of total particles N_{11-470} are presented in Table 2. As previously noted, more than 40% data was lost in December 2001, and the data coverage rates in May 2002 and October 2002 were somewhat lower than other months. The first and second highest mean N_{11-470} were observed during December 2002 and February 2002, respectively. Although the mean number concentration of August was lower than annual average concentration (8160 cm^{-3}), the highest hourly average N_{11-470} was observed at 15:00 (EST) on August 26, 2002, with a maximum value of around 61,440 cm^{-3}.

The monthly variations of N_{11-50} and ambient temperature are shown in Figure 4. Similarly to total concentration, the mean N_{11-50} in winter months (December−February) tended to be higher than the values in summer months (July−August). The highest monthly mean N_{11-50} was found in December 2002 with a mean of 7630 ± 3710 cm^{-3} (mean ± standard deviation) while the mean concentration of July

TABLE 2. Statistical Characteristics of Monthly Averages of Particle Number Concentrations (cm^{-3}) in the Size Range of 0.011−0.470 μm

	mean	median	max	min	SD	valid no.
December 2001	9.20E+03	7.71E+03	4.88E+04	5.41E+02	6.50E+03	420[a]
January 2002	9.21E+03	8.38E+03	2.90E+04	1.08E+03	4.69E+03	594
February 2002	9.92E+03	8.08E+03	3.70E+04	1.47E+03	5.93E+03	658
March 2002	8.92E+03	7.36E+03	3.54E+04	8.65E+02	5.87E+03	700
April 2002	8.70E+03	7.46E+03	5.85E+04	1.44E+03	5.30E+03	711
May 2002	7.41E+03	6.42E+03	4.46E+04	7.20E+02	4.72E+03	562
June 2002	7.35E+03	6.32E+03	5.19E+04	1.55E+03	4.93E+03	671
July 2002	7.03E+03	5.82E+03	5.78E+04	6.10E+02	5.31E+03	732
August 2002	7.38E+03	6.32E+03	6.14E+04	6.20E+02	5.33E+03	744
September 2002	7.48E+03	6.21E+03	4.89E+04	6.00E+02	5.38E+03	637
October 2002	6.67E+03	5.72E+03	2.83E+04	1.14E+03	3.97E+03	549
November 2002	6.95E+03	6.21E+03	2.52E+04	9.50E+02	3.89E+03	720
December 2002	1.01E+04	8.14E+03	5.41E+04	8.30E+02	7.11E+03	711

[a] The data coverage in December 2001 was approximately 56%.

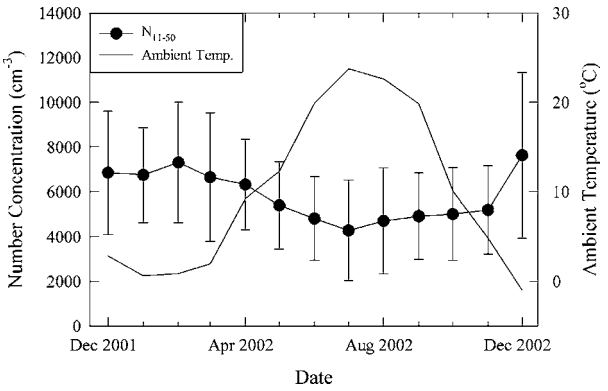

FIGURE 4. Monthly variations of total number concentration and ambient temperature in Rochester, NY. The bars represent standard deviations.

TABLE 3. Hourly Averaged Number Concentrations (cm^{-3}) in the Three Size Ranges during Weekdays and Weekends

diameter (μm)	0.011−0.050	0.050−0.100	0.100−0.470
	Weekday		
mean	6.55E+03	1.52E+03	8.10E+02
median	5.20E+03	1.27E+03	7.10E+02
SD	4.89E+03	1.03E+03	4.80E+02
	Saturday		
mean	5.07E+03	1.44E+03	8.50E+02
median	3.94E+03	1.24E+03	7.30E+02
SD	4.33E+03	1.01E+03	5.50E+02
	Sunday		
mean	3.73E+03	1.32E+03	8.70E+02
median	2.96E+03	1.12E+03	6.90E+02
SD	2.62E+03	9.50E+02	6.65E+02

2002 was lowest with a value of 4280 ± 2250 cm^{-3}. The higher number concentrations of UFP in winter months were probably related to the increased nucleation events of combustion exhaust emitted from motor vehicles as well as lower average mixing heights and inversions that occur more frequently in winter. As shown in Figure 4, the highest monthly average ambient temperature (24 °C) occurred when the monthly average N_{11-50} was lowest, whereas the lowest average ambient temperature (−1 °C) occurred when the highest average number concentration was observed. The mean number concentrations were inversely proportional to ambient temperature. Measurements in an urban atmosphere in Helsinki have shown the similar monthly variation of UFP (*23*). It suggests that ambient temperature is one of the critical factors that affects the dispersion and formation of UFP. However, the highest coefficient of variation was found in July with a value of 52% since the highest hourly concentration and abrupt peaks were typically observed in summer, especially in July although monthly mean N_{11-50} was lower than during winter months.

The comparisons of number concentrations of UFP in the three size ranges during weekdays and weekends are shown in Table 3. Average N_{11-50} during weekdays was significantly higher than the value averaged during weekends by a factor of 1.2−1.7 while the average number concentration was significantly lower on Sundays. In the size range of 0.050−0.100 μm, the number concentrations during weekdays were somewhat higher than the values averaged during weekends, whereas there was no difference in the size range of 0.100−0.470 μm between weekdays and weekends. The results clearly suggest that the number concentrations of UFP are expected to be dominated by local emissions such as motor vehicles, whereas the variations of $N_{100-470}$ are expected to be related to regional sources.

The diurnal variation of number concentrations and standard errors of particles in the three size ranges are presented in Figure 5. In the size range of 0.011−0.050 μm, the first peak usually occurred between 08:00 and 09:00 (EST) with a value of 7700 ± 5390 cm^{-3} (mean ± SD) while the second peak appeared around 15:00 (EST) with a value of 8400 ± 6510 cm^{-3} as the results. The first peak was present at times corresponding to morning rush hours, while the second peak might be related to nucleation events of UFP and to the afternoon rush hour when the mixing heights were higher and the traffic is more spread in time.

Figure 6 shows the diurnal variations of meteorological parameters (ambient temperature, RH, and wind speed) during the same period. Wind speed may be considered as an indicator for a vertical mixing height because the diurnal pattern is similar to the typical variation of the mixing height.

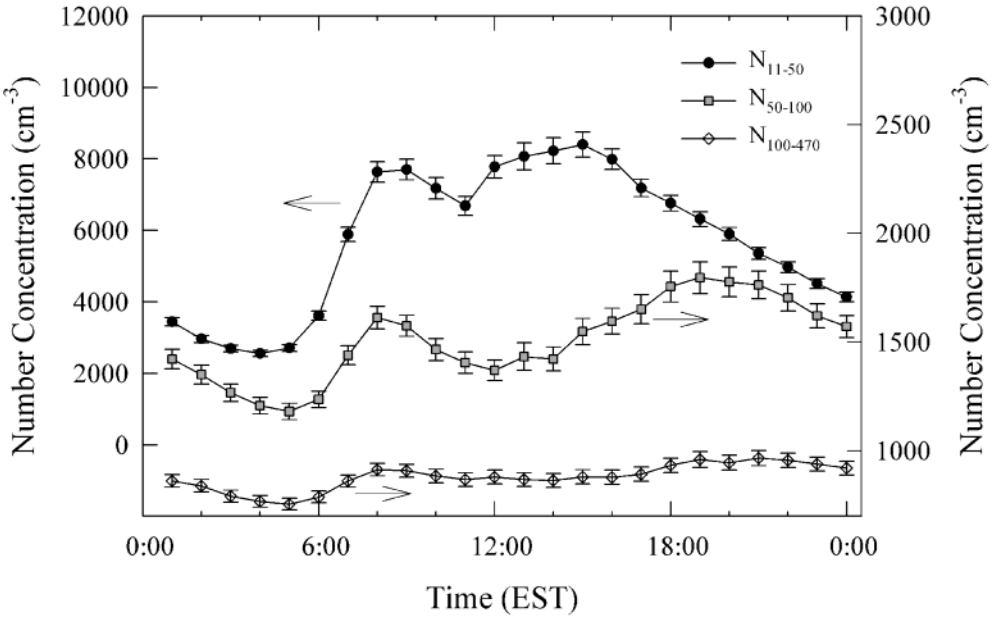

FIGURE 5. Diurnal variations of number concentrations of particles in the three size ranges during the measurement period of December 2001−December 2002. The bars represent standard errors.

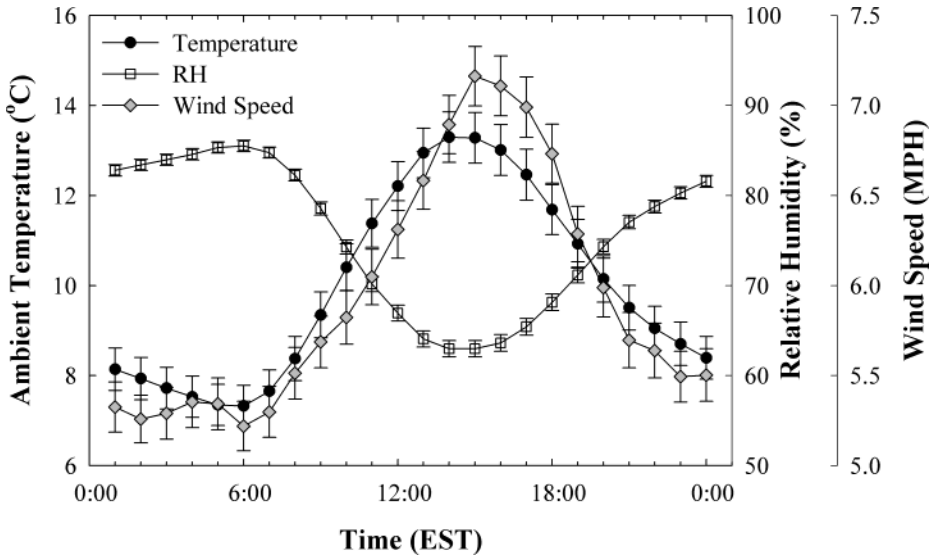

FIGURE 6. Diurnal variations of ambient temperature, relative humidity, and wind speed during the measurement period of December 2001−December 2002. The bars represent standard errors.

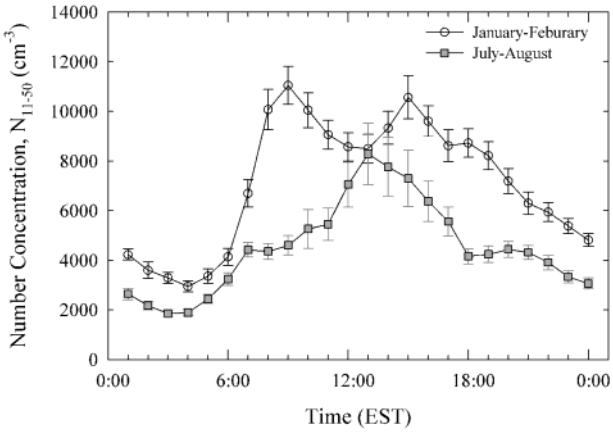

FIGURE 7. Comparison of diurnal variations in ultrafine particles in the size range of 0.011−0.050 μm during winter and summer months. The bars represent standard errors.

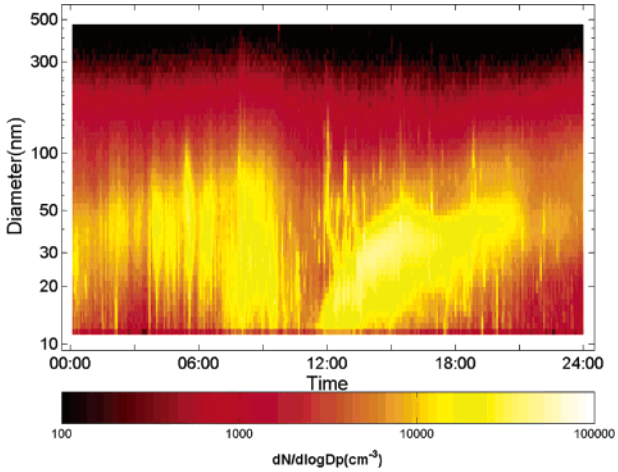

FIGURE 8. Size distributions and number concentrations of ultrafine particles for a typical type of the morning event and the afternoon nucleation event on April 11, 2002.

It appears that the lowest mixing height when wind speed was minimum corresponded to periods of expected high-traffic volume. Thus, the morning UFP peak was the result of motor vehicle emissions combined with a lower mixing layer heights and lower ambient temperature. However, the afternoon peak observed during the maximum wind speed and mixing height period might be more associated with intensity of solar radiation because high ambient temperature and low relative humidity strongly depend on the amount of solar radiation, and nucleation events in the afternoon are likely to occur. The diurnal variations of N_{50-100} were also related to morning rush hour and late evening rush hours as shown in Figure 5. The second peaks in the size range of 0.050−0.100 μm tended to occur after the second peak of N_{11-50}. It might be that the formation of UFP (0.050−0.100 μm) is associated with the coagulation and growth of UFP after evening rush hour. The variation of $N_{100-470}$ was negligible, indicating more regional sources.

Seasonal difference between summer and winter months of the diurnal variation of N_{11-50} is shown in Figure 7. Generally, the concentrations in summer were relatively lower than values in winter months as expected. The trend of diurnal variation in winter was found to be similar to the diurnal variation of N_{11-50} during December 2001−December 2002. In summer the main peak was however observed at around 12:00−13:00, and the morning peak was smaller. The difference can be due to nucleation and higher temperature combined with the higher mixing layer height in summer as mentioned before. The results in Figure 7 shows much higher variations of N_{11-50} at around 13:00 with a value of 8280 ± 9670 cm^{-3} (mean ± SD), suggesting that there were significant new particle formation events in the summer.

Number Concentration and Size Distribution during Nucleation Events. During the measurement period, two peaks of rapid increase in the UFP number concentrations were observed. Figure 8 illustrates the typical pattern of the two types of peaks during a day. The color scale shown in Figure 8 shows the concentration of particles in each size class (in dN/d log D_p). The logarithmic vertical axis is the particle diameter in nanometers, and the horizontal axis is time during the day. The particle number concentrations are shown by the color with highest concentrations being the hottest color. As shown in Figure 8, the first event mostly occurred during morning rush hour (07:00−09:00) with very high concentrations of UFP in the size range of 0.020−0.100 μm (morning events), whereas another event occurred between 12:00 and 18:00 where the dominant particle size tended to be in the 0.011−0.030 μm range (afternoon events).

The morning events were observed throughout the 13-month period, especially in winter months. As can be seen

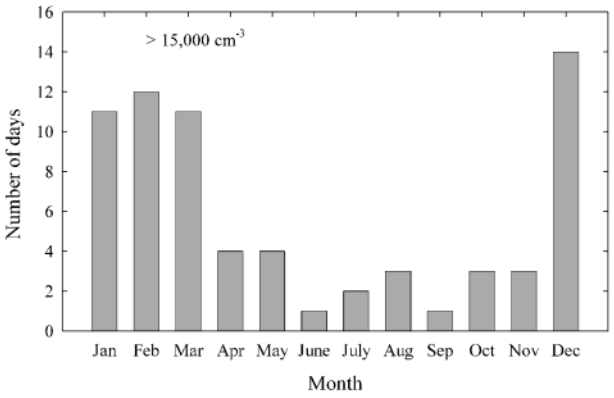

FIGURE 9. Frequency of morning event days with a number concentration of more than 15 000 cm^{-3} during the events in the measurement period.

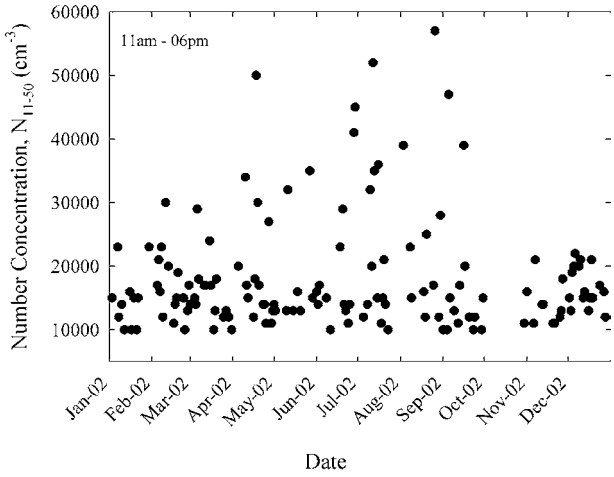

FIGURE 10. Maximum number concentrations of ultrafine particles in the size range of 0.011−0.050 μm during afternoon nucleation events in Rochester, NY.

from Figure 7, the increased number concentrations during the events in winter were higher than the values in summer. The frequency of occurrence of morning events when N_{11-50} was more than 15,000 cm^{-3} is shown in Figure 9. Note that the data for nine days in May and October 2002 were lost due to the malfunction and regular maintenance of a SMPS system, so the nucleation event count might be underestimated for these months. The average number concentration of UFP peaked at around 07:00 and 09:00 for weekdays increased with a mean of approximately 8600 cm^{-3}, whereas the morning events were less commonly observed on weekends. The morning events were most frequently observed in December, and the highest concentration of UFP was approximately 30,000 cm^{-3} at around 09:00 on December 11, 2002. The occurrence frequency of the morning events tended to follow the typical pattern of mixing depths in winter, the season with the lowest mixing depths and wind speeds. CO concentrations were also generally higher during the morning events as might be expected if both arise from the emissions of vehicles with nucleation occurring as the exhaust mixes with the cool ambient air (*35*). It is possible that the morning event represents more formation of UFP by the direct emissions than by photochemical gas-to-particle conversion.

The afternoon events peak at around 12:00 and 18:00 and were observed on 143 d (>10,000 cm^{-3}) out of the total of 335 measurement days during the measurement period of January 2002−December 2002 in Rochester, NY. Figure 10 presents the maximum number concentration of UFP when

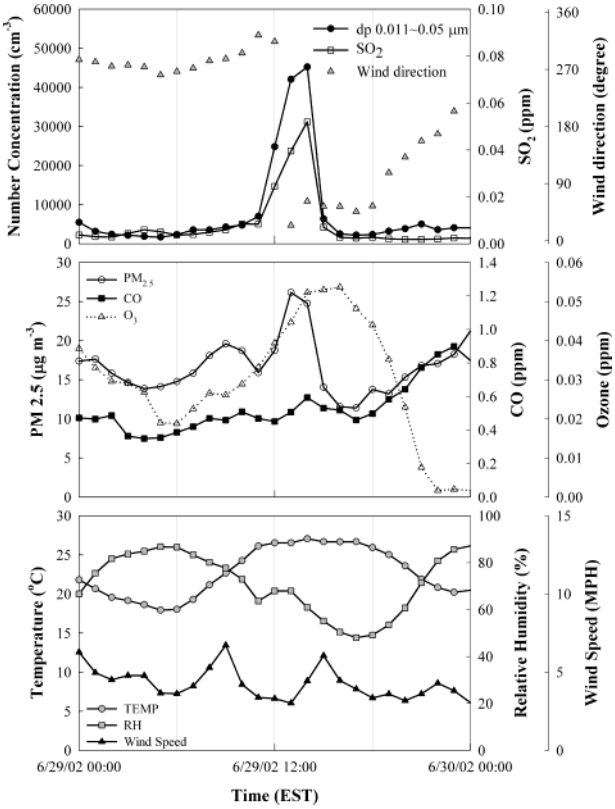

FIGURE 11. Comparison of number concentration, SO_2, CO, O_3, $PM_{2.5}$ mass, wind direction, and wind speed during an ultrafine nucleation event on June 29, 2002.

the afternoon nucleation events were occurring between 11:00 and 18:00. During the afternoon nucleation events, the number concentrations were increased by factors ranging from 10 to 60 from typical values of a few thousand per cubic centimeter. As shown in Figure 10, there was no distinct seasonal variation of the occurrence frequency of the afternoon events. However, strong afternoon events with number concentrations of more than 30,000 cm^{-3} were frequently observed in spring and summer, April through September, and there was only one strong nucleation event in February 2002.

Typical cases of the strong afternoon nucleation events were observed on June 29, 2002, and August 26, 2002, with peak concentration values of 42,000 and 57,000 cm^{-3}, respectively. The variations of N_{11-50}, gaseous pollutants, and meteorological data during these nucleation events are illustrated in Figures 11 and 12. It is noted that since June 28, 2002, was Saturday, the effect of motor vehicles was negligible with no morning traffic peak as shown in Figure 11. In both cases, the nucleation events occurred when ambient temperature was at the maximum for the day and relative humidity ranged from 50% to 70%. The similar trends in the ambient temperature and relative humidity were observed during the nucleation events in summer months. $PM_{2.5}$ mass and CO concentrations were poorly correlated with the UFP number concentrations during the nucleation events (r_s = 0.15 for $PM_{2.5}$, r_s = 0.09 for CO), whereas SO_2 dramatically increased at the same time as the number concentration of particles rose during the nucleation events as can be seen in Figures 11 and 12. The SO_2-related nucleation events were more likely to occur in spring and summer, especially in July with 7 observed days of the 13 afternoon nucleation event days.

To specifically identify the effect of SO_2 on the nucleation events, the observed SO_2-related event days (32 d) of the afternoon nucleation events (74 d) for the period April through

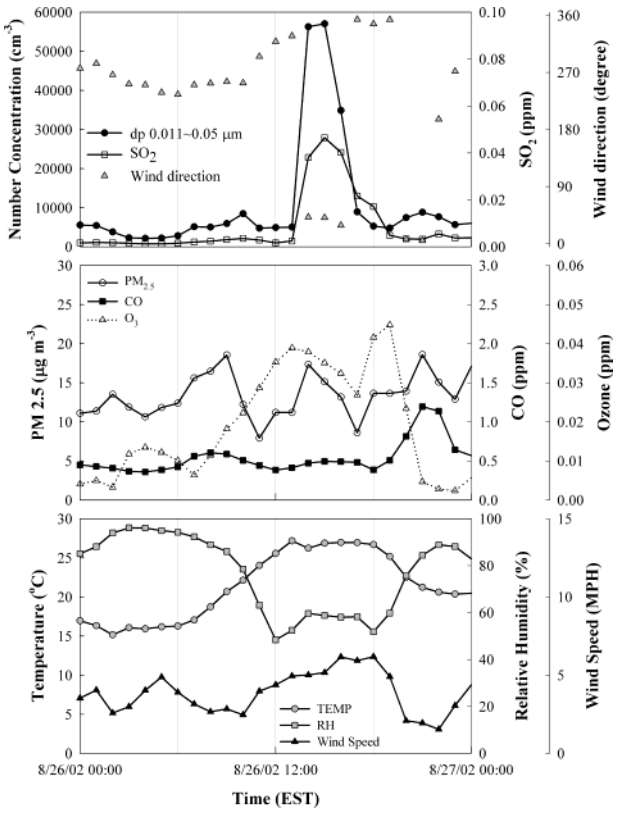

FIGURE 12. Comparison of number concentration, SO_2, CO, O_3, $PM_{2.5}$ mass, wind direction, and wind speed during an ultrafine nucleation event on August 26, 2002.

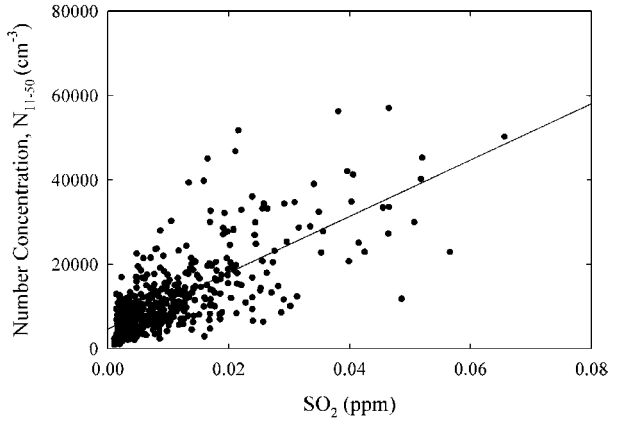

FIGURE 13. Correlation between number concentrations of ultrafine particles and SO_2 concentrations during the afternoon nucleation event from April to September 2002.

September 2002 were extracted from the entire data set (Figure 13). As expected, hourly N_{11-50} was significantly associated with SO_2 during the SO_2-related nucleation days ($r_s = 0.83$) while the Spearman correlation coefficient during all afternoon nucleation events was 0.62. However, during the cooler months except the months from April to September, the SO_2-related nucleation events were found on 6 days among the 69 afternoon nucleation events, and the correlation between N_{11-50} and SO_2 during the afternoon events in the winter months was lower ($r_s = 0.39$). In addition, it appears that 15 strong afternoon events (>30,000 cm^{-3} in the size range of 0.011−0.050 μm) in Figure 10 were surprisingly linked to the SO_2-related nucleation events. These results suggest that the regional pollutant, SO_2, mostly emitted and transported from stationary sources such as coal power plants can affect the afternoon nucleation events occurring

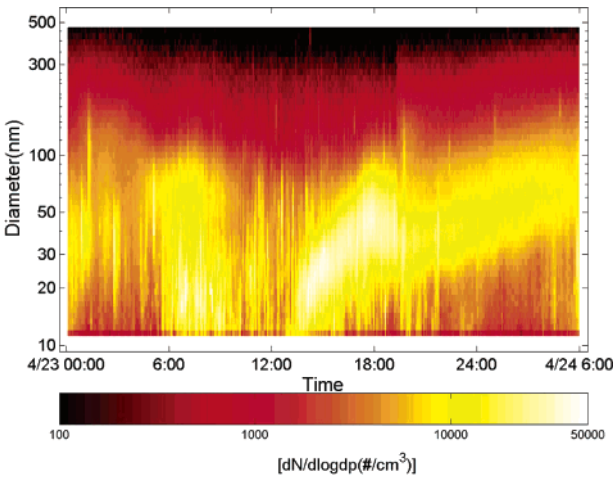

FIGURE 14. Typical growth event observed for 18 h from April 23−24, 2002.

in summer months. The strong peaks of SO_2 were observed when wind direction was northwesterly, where SO_2 sources were located. Long-term measurements of the number concentration of UFP (0.010−0.045 μm) in Atlanta have been shown that SO_2 levels typically increased during nucleation events (*24*, *25*). Birmili and Wiedensohler (*38*) have also found that 80% of significant nucleation events of UFP (0.003−0.011 μm) associated with a SO_2 increase in an urban atmosphere in Germany. Alam al. (*39*) have observed a limited number of nucleation events in Birmingham, UK, and modeling suggests that they were likely to arise from sulfuric acid−water nucleation.

Photochemical reactions oxidizing SO_2 to sulfuric acid and its subsequent nucleation with water and possibly ammonia (NH_3) appear to be primarily responsible for the nucleation events. Ternary nucleation mechanisms (H_2SO_4/H_2O/NH_3) have been proposed as an alternative hypothesis to close discrepancies found between calculated binary H_2SO_4/H_2O nucleation rates and experimental results (*36*). The newly nucleated UFP can be considered as secondary particles formed from the photochemical reaction of SO_2 in the afternoon of summer. Although there was no direct correlation between ozone concentrations and N_{11-50} during the nucleation events, ozone was higher during the events, and higher UV irradiation was likely. The nucleation events seem associated with high solar radiation. This is consistent with observation of Pirjola et al. (*37*), who reported that the strength of the nucleation event increased as a function of UV-B irradiation penetrating into the troposphere and stimulating the SO_2 oxidation process.

There were two types of afternoon nucleation patterns. One type of event involves only nucleation in the size range of 0.011−0.030 μm. The other type begins with nucleation followed by particle growth up to approximately 0.1 μm throughout the late afternoon and evening. As can be seen in the banana shape present in Figure 14, the particle growth event persisted for 18 h. The particles grew to approximately 0.1 μm in diameter following the nucleation around noon and then disappeared at the time of the next morning events at around 07:00 (EST). The growth events were more clearly observed in spring and summer, especially in April. Mäkelä et al. (*21*) observed nucleation and the subsequent growth events for up to the order of 12 h up to around 0.07 μm in Finland. Over the period of 13 months, the observed growth rates of UFP (0.011−0.050 μm) ranged from 0.005 to 0.013 μm/h with a mean of 0.008 μm/h. Studies on newly formed particles have shown that the growth rates of particles (0.003−0.011 μm) at an urban site and at a rural site in Germany were approximately 0.004 and 0.002 μm/h, respectively (*38*,

40). During the growth events, average relative humidity and ambient temperature were approximately 53% and 17 °C, respectively, while main wind direction was southwest with an average wind speed of 3 m/s. In general, steady wind direction was responsible for the effective growth of UFP, whereas wind speed had little effect.

Acknowledgments

This work was supported in part by the New York State Energy Research and Development Authority (NYSERDA) Contract 6820 and by the U.S. Environmental Protection Agency Science to Achieve Results Program through a subcontract from the University of Rochester PM and Health Center supported through STAR Grant R827453. We would like to thank Henry D. Felton of the New York State Department of Environmental Conservation for providing meteorological and gaseous pollutant data.

Literature Cited

(1) Dockery, D. W.; Pope, C. A.; Xu, X.; Spengler, J. D.; Ware, J. H.; Fay, M. E.; Ferris, B. G.; Speizer, F. E. *N. Engl. J. Med*. **1993**, *329*, 1753−1759.

(2) Pope, C. A.; Thun, M. J.; Namboodiri, M. M.; Dockery, D. W.; Evans, J. S.; Speizer, F. E.; Heath, C. W. *Am. J. Respir. Crit. Care Med*. **1995**, *151*, 669−674.

(3) Schwartz, J.; Dockery, D. W.; Neas, L. M. *J. Air Waste Manage. Assoc.* **1996**, *46*, 927−939.

(4) Oberdörster, G.; Ferin, J.; Lehnert, B. E. *Environ. Health Perspect*. **1994**, *102* (Suppl. 5), 173−179.

(5) Seaton, A.; MacNee, W.; Donaldson, K.; Godden, D. *Lancet* **1995**, *345*, 176−178.

(6) Donaldson, K.; Li, X. Y.; MacNee, W. *J. Aerosol Sci.* **1998**, *29*, 553−560.

(7) Oberdörster, G.; Utell, M. J. *Environ. Health Perspect*. **2002**, *110*, A440−441.

(8) Pekkanen, J.; Timonen, K. L.; Ruuskanen, J.; Reponen, A.; Mirme, A. *Environ. Res.* **1997**, *74*, 24−33.

(9) Peters, A.; Wichmann, H. E.; Tuch, T.; Heinrich, J.; Heyder, J. *Am. J. Respir. Crit. Care Med*. **1997**, *155*, 1376−1383.

(10) Wichmann, H. E.; Spix, C.; Tuch, T.; Woelke, G.; Peters, A.; Heinrich, J.; Kreyling, W. G.; Heyder, J. *Health Effects Institute Research Report 98*; 2000.

(11) Penttinen, P.; Timonen, K. L.; Tiittanen, P.; Mirme, A.; Ruuskanen, J.; Pekkanen, J. *Eur. Respir. J.* **2001**, *17*, 428−435.

(12) Pekkanen, J.; Peters, A.; Hoek, G.; Tiittanen, P.; Brunekreef, B.; Hartog, de J.; Heinrich, J.; Ibald-Mulli, A.; Kreyling, W. G.; Lanki, T.; Timonen, K. L.; Vanninen, E. *Circulation* **2002**, *106*, 933−938.

(13) Hughes, L.; Cass, G.; Gone, J.; Ames, M.; Olmez, I. *Environ. Sci. Technol*. **1998**, *32*, 1153−1161.

(14) Harrison, R.; Jones, M.; Collins, G. *Atmos. Environ*. **1999**, *33*, 309−321.

(15) Buzorius, G.; Hämeri, K.; Pekkanen, J.; Kulmala, M. *Atmos. Environ*. **1999**, *33*, 553−565.

(16) Keywood, M. D.; Ayers, G. P.; Gras, J. L.; Gillett, R. W.; Cohen, D. D. *Atmos. Environ*. **1999**, *33*, 2907−2913.

(17) Ruellan, S.; Cachier, H. *Atmos. Environ*. **2001**, *35*, 453−468.

(18) Shi, J. P.; Evans, D. E.; Khan, A. A.; Harrison, R. M. *Atmos. Environ*. **2001**, *35*, 1193−1202.

(19) Watson, J. G.; Chow, J. C.; Lowenthal, D. H.; Stolzenburg, M. R.; Kreisberg, N. M.; Hering, S. V. *J. Air Waste Manage. Assoc*. **2002**, *52*, 822−827.

(20) Weingartner, E.; Nyeki, S.; Baltensperger, U. *J. Geophys. Res*. **1999**, *104*, 26809−26820.

(21) Mäkelä, J. M.; Aalto, P.; Jokinen, V.; Pohja, T.; Nissinen, A.; Palmroth, S.; Markkanen, T.; Seitsonen, K.; Lihavainen, H.; Kulmala, M. *Geophys. Res. Lett*. **1997**, *24*, 1219−1222.

(22) Mäkelä, J. M.; Koponen, I. K.; Aalto, P.; Kulmala, M. *J. Aerosol Sci.* **2000**, *31*, 595−611.

(23) Laakso, L.; Hussein, T.; Aarnio, P.; Komppula, M.; Hiltunen, V.; Viisanen, Y.; Kulmala, M. *Atmos. Environ*. **2003**, *37*, 2629−2641.

(24) Woo, K. S.; Chen, D. R.; Pui, D. Y. H.; McMurry, P. H. *Aerosol Sci. Technol.* **2001**, *34*, 75−87.

(25) McMurry, P. H.; Woo, K. S. *J. Aerosol Med*. **2002**, *15*, 169−178.

(26) Tuch, Th.; Brand, P.; Wichmann, H. E.; Heyder, J. *Atmos. Environ*. **1997**, *31*, 4193−4197.

(27) Ruuskanen, J.; Tuch, Th.; Ten Brink, H.; Peters, A.; Khlystov, A.; Mirme, A.; Kos, G. P. A.; Brunekreef, B.; Wichmann, H. E.; Buzorius, G.; Vallius, M.; Kreyling, W.; Pekkanen, J. *Atmos. Environ*. **2001**, *35*, 3729−3738.

(28) Pakkanen, T. A.; Kerminen, V.-M.; Korhonen, C. H.; Hillamo, R. E.; Aarnio, P.; Koskentalo, T.; Maenhaut, W. *Atmos. Environ*. **2001**, *35*, 4593−4607.

(29) Morawska, L.; Thomas, S.; Bofinger, N. D.; Wainwright, D.; Neale, D. *Atoms. Environ*. **1998**, *32*, 2461−2478.

(30) Morawska, L.; Jayaratne, E. R.; Mengersen, K.; Jamriska, M.; Thomas, S. *Atmos. Environ*. **2002**, *36*, 4375−4383.

(31) Allen, G.; Sioutas, C.; Koutrakis, P.; Reiss, R.; Lurmann, F. W.; Robert, P. T. *J. Air Waste Manage. Assoc.* **1997**, *47*, 682−689.

(32) Ayers, G. P.; Keywood, M. D.; Gras, J. L. *Atmos. Environ*. **1999**, *33*, 3717−3721

(33) Solomon, P. A.; Salmon, L. G.; Fall, T.; Cass, G. R. *Environ. Sci. Technol.* **1992**, *26*, 1594−1601.

(34) Hering, S.; Cass, G. *J. Air Waste Manage. Assoc.* **1999**, *49*, 725−733.

(35) Shi, J. P.; Harrison, R. M. *Environ. Sci. Technol*. **1999**, *33*, 3730−3736.

(36) Korhonen, P.; Kulmala, M.; Laaksonen, A.; Viisanen, Y.; McGraw, R.; Seinfeld, J. H. *J. Geophys. Res.* **1999**, *104*, 26349−26353.

(37) Pirjola, L.; Kulmala, M.; Wilck, M.; Bischoff, A.; Stratmann, F.; Otto, E. *J. Aerosol Sci*. **1999**, *30*, 1079−1094.

(38) Birmili, W.; Wiedensohler, A. *Geophys. Res. Lett*. **2000**, *27*, 3325−3328.

(39) Alam, A.; Shi, J. P.; Harrison, R. M. *J. Geophys. Res.* **2003**, *108*, art. no. 4093.

(40) Birmili, W.; Wiedensohler, A.; Plass-Dülmer, C.; Berrresheim, H. *Geophys. Res. Lett*. **2000**, *27*, 2205−2208.

Received for review July 23, 2003. Revised manuscript received December 12, 2003. Accepted January 6, 2004.

ES034811P